

# Improved computed radiography image quality from a BaFI:Eu photostimulable phosphor plate

Yasushi Nakano, Tomonori Gido, Satoshi Honda, Akihiro Maezawa, Hideaki Wakamatsu, and Takafumi Yanagita

*MG Imaging R&D Center, Konica Corporation, No. 1 Sakura-machi, Hino-shi, Tokyo 191-8511, Japan*

(Received 25 January 2001; accepted for publication 3 January 2002; published 21 March 2002)

Recent advances in the design of photostimulable phosphor (PSP) plates for computed radiography (CR) systems have made it possible to manufacture plates made of BaFI:Eu phosphor material in the cassette form. The image quality of this plate, six BaF(Br,I):Eu plates, and one BaFBr:Eu plate were evaluated in terms of presampling modulation transfer function (MTF), normalized Wiener spectra ( $WS_N$ ), and detective quantum efficiency (DQE). Compared with the best-performing BaF(Br,I):Eu plate, the BaFI:Eu plate provided DQE that was higher, at spatial frequencies of 0.5, 1.0, and 2.0 cycles/mm, by 12% (21.8 versus 19.4), 13% (18.8 versus 16.7), and 11% (12.0 versus 10.8), respectively. Since presampling MTF values of the two plates were comparable, the BaFI:Eu plate's higher DQE is attributable to total  $WS_N$  conversely being lower by 17% [ $8.65 \times 10^{-5}$  ( $\text{mm}^2$ ) versus  $10.38 \times 10^{-5}$  ( $\text{mm}^2$ )], 17% [ $5.85 \times 10^{-5}$  ( $\text{mm}^2$ ) versus  $7.03 \times 10^{-5}$  ( $\text{mm}^2$ )], and 12% [ $2.82 \times 10^{-5}$  ( $\text{mm}^2$ ) versus  $3.19 \times 10^{-5}$  ( $\text{mm}^2$ )] at the specified frequencies, respectively, primarily due to the contribution of x-ray quantum  $WS_N$ . This jibes with the high x-ray absorption provided by the 27%-higher x-ray attenuation coefficients (7.54 versus 6.07, at 60 KeV) that BaFI offers over BaF( $\text{Br}_{0.85}, \text{I}_{0.15}$ ), a result of the high atomic number of BaFI's exclusively iodine halide content. The results were consistent with earlier studies of several of these same plates and indicate that BaFI:Eu is a promising avenue to lower image noise and higher overall CR system image quality. © 2002 American Association of Physicists in Medicine. [DOI: 10.1118/1.1462639]

Key words: computed radiography, detective quantum efficiency, photostimulable phosphor, total normalized WS, x-ray absorption

## I. INTRODUCTION AND BACKGROUND

Since the debut of computed radiography (CR) in the early 1980s, several BaFX compounds have been used in the photostimulable phosphor (PSP) plates of CR systems,<sup>1</sup> the latest of which is BaFI:Eu. To ascertain the place of this new BaFX in the array of BaFX PSPs historically used in CR, we examined this BaFI:Eu plate (Konica RP-1S) along with seven other PSP plates that span the generations of CR systems (Table I), including five from Fuji's ST series and one each from Kodak (GP-25) and Agfa (MD-10). We evaluated and compared the sharpness, image noise, and overall image quality of the eight plates in terms of presampling modulation transfer function (MTF), normalized Wiener spectra ( $WS_N$ ), and detective quantum efficiency (DQE).

A brief sketch of the technology and history that led to this study may aid those for whom these are unfamiliar. A CR system's PSP plate is critical to its x-ray image quality, two major aspects of which are sharpness and image noise. Image quality can be quantified as DQE, and sharpness and image noise can be quantified as presampling MTF and total  $WS_N$ , respectively. Presampling MTF depends chiefly on laser light scattering in the PSP plate, which, in turn, depends upon the physical qualities of plate materials and construction. Total  $WS_N$  (WS divided by the square of the mean value, and perceived in the image as mottle) has three components: structure  $WS_N$ , luminescence  $WS_N$ , and x-ray quantum  $WS_N$ .

Structure  $WS_N$  increases with irregularities in the plate's laser-induced photostimulable luminescence (PSL) emissions, which stem from such conditions as inconsistent thickness of the PSP layer, lack of PSP layer surface flatness, and uneven distribution of PSP particles. Luminescence  $WS_N$  increases when the PSL, which functions as a signal carrier, decreases in intensity, thus lowering the signal-to-noise ratio. PSL intensity is affected by PSP particle size, by the amount of dopant present, and especially by impurities in the PSP material.

Of greatest interest to the study here is x-ray quantum  $WS_N$ . X-ray quantum  $WS_N$  increases with a decrease in the image-carrying x-ray quanta absorbed by the PSP plate. Given a maximum practical x-ray dose, the x-ray absorption of the PSP plate is the operative factor here, and both the physical and the chemical natures of the PSP plate come into play. Physically, x-ray absorption can be raised by increasing phosphor layer thickness and/or phosphor particle packing density. However, a phosphor layer can become only so thick before sharpness unacceptably declines, and there are practical limits to how densely phosphor particles can be packed. Chemically, x-ray absorption can be raised by selecting a PSP material that provides relatively high x-ray attenuation coefficients.

This final fact explains the attraction of BaFI:Eu.<sup>2</sup> When CR made its debut in 1982, the original PSP plate (Fuji's ST-I) was a BaFBr:Eu plate,<sup>3,4</sup> but in 1988, the BaF(Br,I):Eu

TABLE I. Computed radiography PSP plates studied.

PSP plate	PSP plate material
ST-I (Fuji)	BaFBr:Eu
ST-III (Fuji)	BaF(Br <sub>0.85</sub> , I <sub>0.15</sub> ):Eu
ST-IIIN (Fuji)	BaF(Br <sub>0.85</sub> , I <sub>0.15</sub> ):Eu
ST-VA (Fuji)	BaF(Br <sub>0.85</sub> , I <sub>0.15</sub> ):Eu
ST-VN (Fuji)	BaF(Br <sub>0.85</sub> , I <sub>0.15</sub> ):Eu
GP-25 (Kodak)	BaF(Br <sub>0.90</sub> , I <sub>0.10</sub> ):Eu
MD-10 (Agfa)	BaF(Br <sub>0.85</sub> , I <sub>0.15</sub> ):Eu
RP-1S (Konica)	BaFI:Eu

plate was introduced (Fuji's ST-III).<sup>1,2</sup> This use of iodine allowed iodine's higher atomic number to increase the x-ray attenuation coefficients of the PSP, thus raising x-ray absorption, and since that initial application, PSP plates of various design have employed BaF(Br,I):Eu. By extension, the ultimate exploitation of iodine in raising x-ray absorption would be a BaFI:Eu (Ref. 2) plate, but this was beyond practical reach until 1998, when obstacles to purity of synthesis and protection from moisture were overcome, and a BaFI:Eu PSP plate (Konica's RP-1S) was introduced in a cassette CR system.

As a cassette CR system, the ability to perform under wide-ranging conditions, i.e., with a great variety of tissue types, is a serious design concern, making very low total  $WS_N$  especially important. Thus, it is highly desirable if low x-ray quantum  $WS_N$  can be achieved by way of the high x-ray absorption provided by BaFI:Eu's significantly higher x-ray attenuation coefficients. For this reason, the comparative study here investigated whether this plate's DQE, total  $WS_N$ , x-ray quantum  $WS_N$ , and other measures of performance were consistent with the gains in x-ray absorption promised by BaFI:Eu's higher x-ray attenuation coefficients.

## II. METHODS

Data was obtained regarding bromine and iodine content, x-ray attenuation coefficients, presampling MTF,  $WS_N$ , and DQE through the following methods.

### A. Bromine and iodine contents

The relative bromine and iodine contents of the PSPs used in the eight PSP plates studied were obtained through wavelength dispersive x-ray (WDX) spectroscopy.<sup>5</sup>

### B. X-ray attenuation coefficients

At x-ray photon energies common to radiography, the values of the x-ray attenuation coefficients,  $\mu/\rho$ , for the BaFX materials used in the PSP plate studied were obtained according to simple additivity

$$\mu/\rho = \sum_i w_i (\mu/\rho)_i, \quad (1)$$

where  $w_i$  is the fraction by weight of the  $i$ th atomic constituent, and the  $(\mu/\rho)_i$  values are taken from Seltzer and Hubbell's tables of mass attenuation coefficients.<sup>3</sup>

### C. Presampling MTF

The presampling MTF of the eight PSP plates were measured using a slit method developed by Fujita *et al.*<sup>6</sup> This method avoids the effects of aliasing on the measured results. The slit test device was made of a 2 mm thick lead piece with a 60 mm long, 10  $\mu$ m wide slit. The images of the slit device were acquired using a positioning system to achieve reproducible positioning of the PSP plates and alignment of the slit opening with respect to the incident x-ray beam. In the acquisitions, the slit device was separated from the plate by 10 mm. The exposures were made using a Toshiba DRX-2903HD x-ray tube with a 1 mm focal spot at 80 kVp, 90 mAs, and a 200 cm source-image distance (SID), and had no added filtration. These technique factors provided an incident exposure of  $3.15 \times 10^{-5}$  C/kg (122 mR).

The slit assembly and the plate cassette faceplate separated the slit from the plate by 10 mm, resulting in a slit magnification not great enough to cause appreciable distortion. Prior to acquiring images, the slit was carefully aligned by means of trial exposures which determined angular positions yielding highest intensities. MTF data was acquired along the subscan direction with the slit positioned horizontally on each PSP plate. To minimize the effects of slit non-uniformity and optimize line spread function (LSF) sampling, the slit was angled 3° from the respective horizontal or vertical.

A 120 second delay was maintained between exposure and reading. To read the slit image, a Konica Regius 150 reader with a pixel size of 87.5  $\mu$ m was used. This same reader was used with all eight plates, achieving mechanical compatibility by mounting the GP-25, MD-10, and the ST series plates on vacant RP-1S plate supports. The absence of any integral plate supports allowed the flexible MD-10 and ST series plates to be mounted directly on the vacant RP-1S plate supports. Because the GP-25 does have an integral plate support, however, this plate had to first be peeled from its support, which was done with deliberate care so as not to damage the plate.

After the image was acquired, the image was sampled every 0.01 mm to obtain a fine-sampled LSF curve. To remove the glare component, the tails of the curve were then truncated and exponentially extrapolated below 2% relative luminance. From the Fourier transform of this extrapolated curve, the presampling MTF was obtained.

### D. $WS_N$

The image noise of the eight PSP plates was compared in terms of total  $WS_N$  and its three components: structure  $WS_N$ , luminescence  $WS_N$ , and x-ray quantum  $WS_N$ .

Following Hillen *et al.*,<sup>7</sup> total  $WS_N$  was obtained under radiographic conditions similar to those of an x-ray of the abdominal region. The resultant use of a single incident exposure,  $3.46 \times 10^{-8}$  C/kg (0.134 mR), placed limits on the results, but this exposure was chosen because it simulates a common situation in medical radiography.

A Toshiba DRX-2903HD x-ray tube was used at exposure conditions of 80 kVp and 1.2 mAs, with an incident expo-

measure of  $3.46 \times 10^{-8}$  C/kg (0.134 mR). Added filtration consisted of a 0.5 mm thick Cu plate and a 4.0 mm thick Al plate, and the SID was 200 cm. A Konica Regius 150 reader with a pixel size of  $87.5 \mu\text{m}$  was again used, and mechanical compatibility between the reader and the PSP plates was achieved in the same manner as with MTF measurement.

Each plate was uniformly exposed, read with the reader, and then subjected to a one-dimensional slit synthesis method to analyze the resultant flat field image. A sampling slit  $87.5 \mu\text{m}$  wide and 3.15 mm long (i.e.,  $1 \times 36$  pixels) was used to scan 1024 pixels across the image, and the slit data from these samplings was then averaged to obtain 1D data. After eliminating the effects of low-frequency nonuniformity (i.e., heel effect), the resultant pixel data was converted, first, to PSL intensity and then, by means of fast Fourier transform, to Fourier spectrum data. Finally, the following equation was applied:

$$WS_N(u) = |F(u)|^2 \frac{(3.15 \text{ mm})}{1024 \times 87.5 \times 10^{-3} \text{ mm}} \quad (2)$$

where  $WS_N(u)$  is the normalized Wiener spectrum at a given spatial frequency,  $F(u)$  is Fourier spectrum at a given frequency, 3.15 mm is the slit length, and  $1024 \times 87.5 \times 10^{-3}$  mm is the scan length, i.e., the product of pixel number (1024) and pixel size ( $87.5 \times 10^{-3}$  mm). Slit length was divided by scan length in order to normalize the WS data, and the  $WS_N$  values were confirmed not to depend on slit length. By repeating this 1D process down the image from top to bottom, and then integrating the  $WS_N$  data from each line, overall  $WS_N$  for the flat field image was obtained.

To obtain structure  $WS_N$ , each PSP plate was re-examined under conditions identical to those under which total  $WS_N$  was obtained, with two exceptions: the tube output was increased to 200 mAs and the incident exposure to  $7.74 \times 10^{-6}$  C/kg (30.0 mR). These extreme conditions revealed the structure  $WS_N$  component of total  $WS_N$  by minimizing the relative contributions of luminescence  $WS_N$  and x-ray quantum  $WS_N$ .

With total  $WS_N$  and structure  $WS_N$  now determined, luminescence  $WS_N$  and x-ray quantum  $WS_N$  were calculated by taking advantage of the fact that luminescence  $WS_N$  is equal at all spatial frequencies and by applying the earlier measured presampling MTF values to express x-ray quantum  $WS_N$ . Based on Hillen,<sup>7</sup> the equation used was

$$WS_N = \frac{1}{(\alpha Gn)} + \frac{MTF^2(u)}{(\alpha n)} \quad (3)$$

where  $\alpha$  is the fractional x-ray absorption of the PSP plate,  $G$  is the PSL output of the PSP plate,  $n$  is the number of x-ray quanta, and where, further,  $1/(\alpha Gn)$  expresses luminescence  $WS_N$  and  $MTF^2(u)/(\alpha n)$  expresses x-ray quantum  $WS_N$ . By using two sets of data corresponding to spatial frequencies of 2.0 cycles/mm and 5.0 cycles/mm, luminescence  $WS_N$  and x-ray quantum  $WS_N$  were able to be calculated.

## E. DQE

DQE, which provided a composite view of sharpness and image noise, was calculated from presampling MTF and  $WS_N$  values, using the following equation, based on Hillen:<sup>7</sup>

$$DQE = \frac{MTF^2(u)}{q(3.46 \text{ C kg}^{-1})[\text{Total } WS_N(u)]}, \quad (4)$$

where  $q$  is  $1.12 \times 10^{12}$  photon  $\text{mm}^{-2} \text{C}^{-1} \text{kg}$ .

To determine this  $q$  value, Seltzer and Hubbell<sup>8</sup> were followed and the x-ray attenuation coefficients were obtained for the total of the added filtration of 0.5 mm Cu and 4.0 mm Al, and the x-ray tube's internal filtration of 2.0 mm Al. Then, following Birch, Marshall, and Ardran,<sup>9</sup> the x-ray attenuation coefficient data for the total filtration were applied to obtain the attenuated relative kerma spectrum in KeV. At increments of 1.0 KeV, the ratio of the attenuated relative kerma value at each increment to the total of those incremental values across the kerma spectrum was determined. At each increment, the corresponding photon-to-kerma-in-air conversion factor was also converted (at  $1 \mu\text{Gy} = 0.115 \text{ mR}$ ) from  $\mu\text{Gy} \times \text{photon}^{-1} \times \text{mm}^2$  to  $\text{mR} \times \text{photon}^{-1} \times \text{mm}^2$ . The inverse of this photon-to-kerma-in-air conversion factor (i.e.,  $\text{photon} \times \text{mR}^{-1} \times \text{mm}^2$ ) was then multiplied by the earlier determined ratio of relative kerma value to total relative kerma values. The total of this product for all increments was the  $q$  value.

## III. RESULTS AND DISCUSSION

A comparison of the image quality of the eight PSP plates in terms of presampling MTF,  $WS_N$ , and DQE indicated that the high x-ray attenuation coefficients of BaFI:Eu succeeded in lowering image noise and raising overall CR system image quality.

### A. Bromine and iodine contents

The relative bromine and iodine contents of the PSPs used in the eight PSP plates studied are found in Table I. Notable was that the iodine content in the BaF(Br, I):Eu PSP plates studied were limited to 15 mol% of iodine or less (note GP-25's 10 mol% of iodine).

### B. X-ray attenuation coefficients

X-ray attenuation coefficients did rise with the introduction of iodine, but the gain obtained with BaF(Br, I):Eu was marginal when compared with the exclusively iodine halide content of BaFI:Eu [Fig. 1: the curve for BaF(Br<sub>0.90</sub>, I<sub>0.10</sub>) is omitted because it would be indistinguishable here from that of BaF(Br<sub>0.85</sub>, I<sub>0.15</sub>)]. While the x-ray attenuation coefficients of the BaF(Br, I):Eu plates are higher than those of BaFBr, the x-ray attenuation coefficients of BaFI are higher still, and by a substantial margin. For example, at 60 KeV, the x-ray attenuation coefficient of BaFI (7.54) is 24% higher than that of BaF(Br<sub>0.85</sub>, I<sub>0.15</sub>) (6.07), 27% higher than that of BaF(Br<sub>0.90</sub>, I<sub>0.10</sub>) (5.92), and 29% higher than that of BaFBr (5.83).

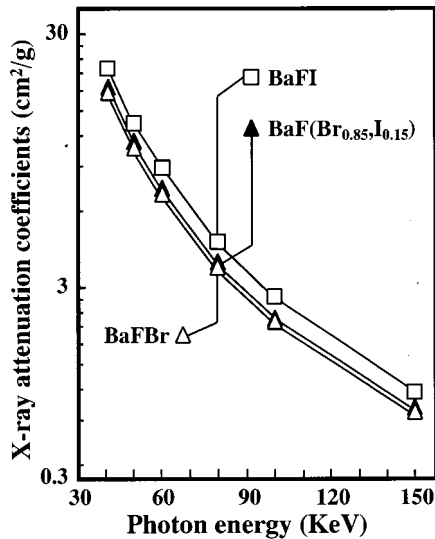


FIG. 1. X-ray absorption coefficients of BaFBr, BaF(Br<sub>0.85</sub>, I<sub>0.15</sub>), and BaFI.

**C. Presampling MTF and sharpness**

We found that the presampling MTF curves of the PSP plates ran closely together, although ST-IIIIN's lower presampling MTF was somewhat exceptional (Fig. 2). It is not established that this historically standard range of presampling MTF curves fully satisfies the diagnostician's demand for CR image sharpness, although defining a range of presampling MTF curves that does so would be of considerable interest in CR system design. For if the presampling MTF curves of a PSP plate need not be raised above an acceptable range, then advantage can be taken of the tradeoff between greater sharpness and lower image noise to minimize the latter. At any rate, the presampling MTF curves we obtained suggested roughly equivalent sharpness among the plates studied.

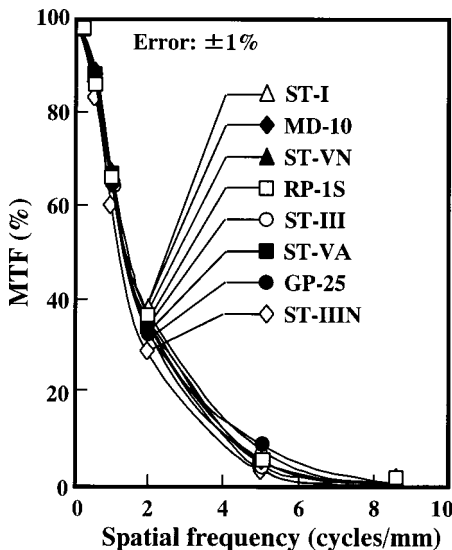


FIG. 2. Presampling MTF of PSP plates evaluated. X-ray tube set at 80 kVp, no added filtration.

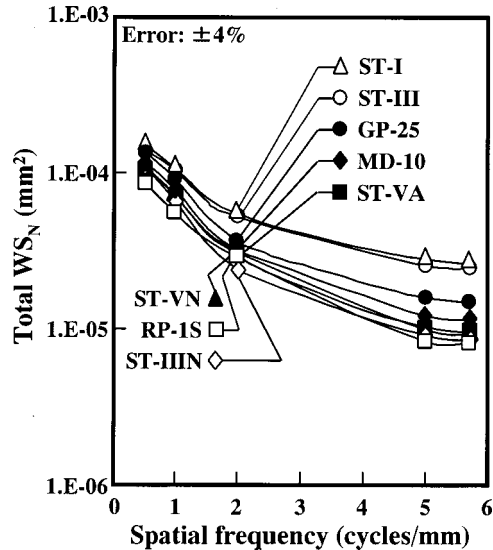


FIG. 3. Total normalized Wiener spectrum ( $WS_N$ ) of PSP plates evaluated. X-ray tube set at 80 kVp, with an incident exposure of  $3.46 \times 10^{-8}$  C/kg (0.134 mR) and added filtration consisting of a 0.5 mm thick Cu plate and a 4.0 mm thick Al plate.

**D.  $WS_N$  and image noise**

In terms of total  $WS_N$ , the newer generation PSP plates fared better than the older (Fig. 3), not surprising in view of the progress that continues to mark CR technology in general. As with our presampling MTF results, the exception again was ST-IIIIN, whose low total  $WS_N$  was especially evident in the vicinity of 2.0 cycles/mm. Regardless, the basic trend toward lower image noise was clear, and of interest to our comparative study was that the BaFI:Eu plate, RP-1S, showed relatively low total  $WS_N$  across all frequencies. For example, in comparison with ST-VN (whose DQE would later prove to most closely approximate that of RP-1S), the total  $WS_N$  of the RP-1S image at 0.5 cycles/mm was 17% lower [ $8.65 \times 10^{-5}$  ( $mm^2$ ) versus  $10.38 \times 10^{-5}$  ( $mm^2$ )]; at 1.0 cycles/mm, it was 17% lower [ $5.85 \times 10^{-5}$  ( $mm^2$ ) versus  $7.03 \times 10^{-5}$  ( $mm^2$ )]; and at 2.0 cycles/mm, it was 12% lower [ $2.82 \times 10^{-5}$  ( $mm^2$ ) versus  $3.19 \times 10^{-5}$  ( $mm^2$ )].

Because total  $WS_N$  is the sum of structure  $WS_N$ , luminescence  $WS_N$ , and x-ray quantum  $WS_N$ , we examined each of these components in order to determine the source of the progress we had observed in total  $WS_N$ . The results we obtained and the relationships among these four measures of  $WS_N$  for each PSP plate are typified by RP-1S (Fig. 4). For all eight PSP plates at this incident exposure of  $3.46 \times 10^{-8}$  C/kg (0.134 mR), structure  $WS_N$  remained a negligible component of total  $WS_N$  across the full range of spatial frequencies examined. Any differences in total  $WS_N$  we observed within this range of spatial frequencies could thus be ascribed chiefly to one or both of the latter two components.

Just as RP-1S's four measures of  $WS_N$  exemplify the minimal influence of structure  $WS_N$ , they also exemplify the role of luminescence  $WS_N$ . For all eight PSP plates at this incident exposure, the effect of luminescence  $WS_N$  was significant, especially at high spatial frequencies, since lumines-

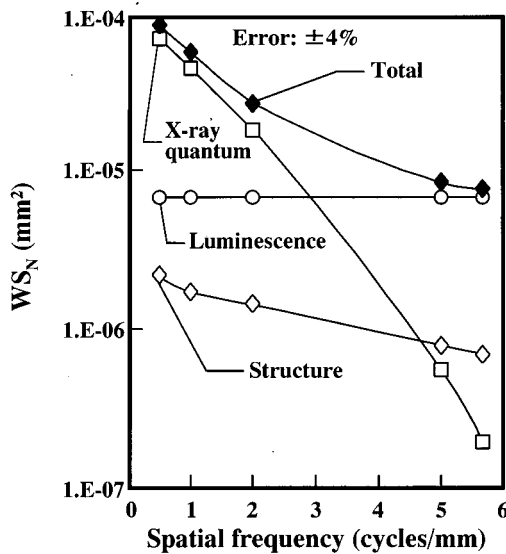


FIG. 4. Total normalized Wiener spectrum ( $WS_N$ ) and its three components illustrated by RP-1S. X-ray tube set at 80 kVp, with an incident exposure of  $3.46 \times 10^{-8}$  C/kg (0.134 mR) and added filtration consisting of a 0.5 mm thick Cu plate and a 4.0 mm thick Al plate.

cence  $WS_N$  does not diminish with spatial frequency. But even for the older PSP plates, luminescence  $WS_N$  did not account for half of total  $WS_N$  until approaching a spatial frequency of 3.0 cycles/mm (Fig. 4), and in the spatial frequency range of 0.5 to 2.0 cycles/mm, the luminescence  $WS_N$  of all eight PSP plates was a significant, but clearly secondary, component of total  $WS_N$ . To continue the earlier comparison with ST-VN, the luminescence  $WS_N$  of the RP-1S image was again somewhat lower (Fig. 5); across the range of spatial frequencies, it was 9% lower [ $7.37 \times 10^{-6}$  ( $mm^2$ ) versus  $8.14 \times 10^{-6}$  ( $mm^2$ )], but the RP-1S

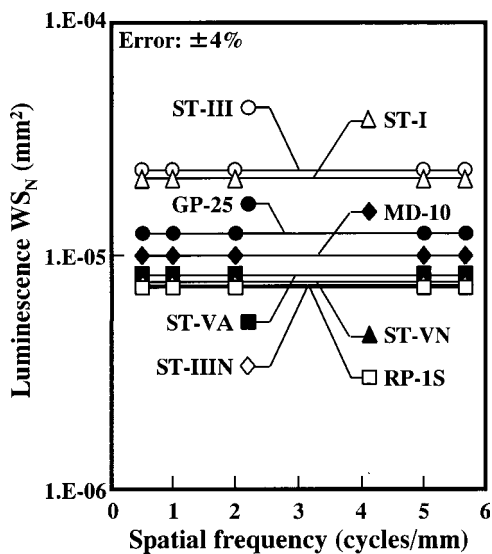


FIG. 5. Luminescence normalized Wiener spectrum ( $WS_N$ ) of PSP plates evaluated. X-ray tube set at 80 kVp, with an incident exposure of  $3.46 \times 10^{-8}$  C/kg (0.134 mR) and added filtration consisting of a 0.5 mm thick Cu plate and a 4.0 mm thick Al plate.

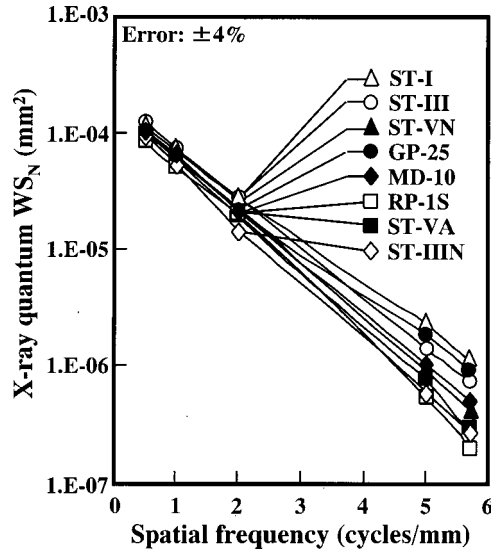


FIG. 6. X-ray quantum Wiener spectrum ( $WS_N$ ) of PSP plates evaluated. X-ray tube set at 80 kVp, with an incident exposure of  $3.46 \times 10^{-8}$  C/kg (0.134 mR) and added filtration consisting of a 0.5 mm thick Cu plate and a 4.0 mm thick Al plate.

and the ST-VN plates were both among the cluster of four PSP plates whose luminescence  $WS_N$  was lowest. Since only one component of total  $WS_N$  remained to be examined, the root of the differences in total  $WS_N$  between RP-1S and ST-VN would predictably be found in that component: x-ray quantum  $WS_N$ .

Whereas, in the spatial frequency range of 0.5 to 2.0 cycles/mm, structure  $WS_N$  was negligible and luminescence  $WS_N$  was secondary, x-ray quantum  $WS_N$  proved to be the primary component of total  $WS_N$  in all eight plates (Fig. 6). Once again, the only unusual finding involved ST-IIIN, whose low x-ray quantum  $WS_N$  was predictable on the basis of its low total  $WS_N$ , but was also at odds with the comparatively low x-ray attenuation coefficients of its PSP, BaF(Br<sub>0.85</sub>, I<sub>0.15</sub>). Just as for ST-IIIN's presampling MTF, we cannot account for this, but we discovered no other puzzling results, RP-1S exhibited very low x-ray quantum  $WS_N$ , and in continuing the comparison with ST-VN, we found that the x-ray quantum  $WS_N$  of the RP-1S image at 0.5 cycles/mm was 18% lower [ $7.68 \times 10^{-5}$  ( $mm^2$ ) versus  $9.41 \times 10^{-5}$  ( $mm^2$ )]; at 1.0 cycles/mm, it was 19% lower [ $4.92 \times 10^{-5}$  ( $mm^2$ ) versus  $6.09 \times 10^{-5}$  ( $mm^2$ )]; and at 2.0 cycles/mm, it was 15% lower [ $1.93 \times 10^{-5}$  ( $mm^2$ ) versus  $2.26 \times 10^{-5}$  ( $mm^2$ )]. This not only jibed with the prediction that their differences in total  $WS_N$  might be traced to differences in x-ray quantum  $WS_N$ , but was also consistent with the higher x-ray absorption provided by BaFI:Eu's higher x-ray attenuation coefficients.

**E. DQE and overall image quality**

Our DQE findings (Fig. 7) confirmed a rough, inverse correspondence between total  $WS_N$  and DQE. That the correspondence exists is consistent with the fact that the pre-

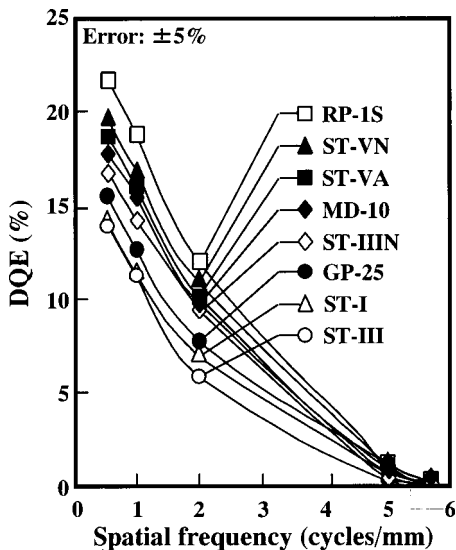


FIG. 7. DQE of PSP plates evaluated, calculated from presampling MTF and Wiener spectrum ( $WS_N$ ). Presampling MTF was obtained with x-ray tube set at 80 kVp and with no added filtration. Total normalized Wiener spectrum ( $WS_N$ ) was obtained with x-ray tube set at 80 kVp, with an incident exposure of  $3.46 \times 10^{-8}$  C/kg (0.134 mR), and with added filtration consisting of a 0.5 mm thick Cu plate and a 4.0 mm thick Al plate.

sampling MTFs of the plates did not differ greatly; that the correspondence is rough is consistent with the fact that the presampling MTFs did, nevertheless, differ.

Further, we found that RP-1S, with its lowest total  $WS_N$ , also had the highest DQE values across the entire range of spatial frequencies examined, and especially so in the lower portion of this range. In final comparison with ST-VN, the best-performing BaF(Br, I):Eu plate, RP-1S displayed DQE that was 12% higher (21.77 versus 19.41) at 0.5 cycles/mm, 13% higher (18.82 versus 16.67) at 1.0 cycles/mm, and 11% higher (11.98 versus 10.76) at 2.0 cycles/mm.

Finally, we compared our DQE findings with those of several studies<sup>10–12</sup> which had previously compared the DQE values of several of the same PSP plates that we ourselves evaluated. Like Dobbins *et al.*<sup>10</sup> we found that ST-IIIN had higher DQE values than ST-III. Like Bradford, Peppler, and Dobbins,<sup>11</sup> we found that ST-IIIN had higher DQE values than GP-25. And, like Kengyelics,<sup>12</sup> we too found that ST-VN had higher DQE values than ST-VA. Although the methodologies of these studies differed somewhat from each other and from our own, the consistency of their findings with our own was encouraging.

#### IV. SUMMARY AND CONCLUSION

To summarize, we found the following:

- (1) That the BaFI:Eu PSP plate had DQE superior to the BaF(Br, I):Eu and BaFBr:Eu plates examined.
- (2) That since the presampling MTF performance of all the PSP plates was comparable, this higher DQE resulted from lower total  $WS_N$ .

- (3) Further, that since the effects of structure  $WS_N$  at the exposure levels evaluated were negligible, and those of luminescence  $WS_N$  were secondary, this lower total  $WS_N$  was attributable to lower x-ray quantum  $WS_N$ .
- (4) That, although we did not directly investigate the mechanism, the BaFI:Eu PSP plate's lower x-ray quantum  $WS_N$  is most plausibly explained by the higher x-ray absorption furnished by the higher x-ray attenuation coefficients that are gained from the exclusively iodine halide content of BaFI:Eu.
- (5) That, in conclusion, the selection of a PSP plate material possessing high x-ray attenuation coefficients, such as BaFI:Eu, is a promising avenue to lower image noise and higher overall CR system image quality.

#### ACKNOWLEDGMENTS

The authors are grateful for the invaluable logistical support of Hisashi Yamaguchi, Haruhiko Masutomi, and Hisanori Tsuchino, and for the exceptional assistance of George E. Reseter.

- <sup>1</sup> K. Takahashi, "Kijinsei keikotai o mochita imeijingu shisutemu" ("Imaging systems using photostimulable phosphors"), Phosphor Research Society (of Japan) 240th Meeting Technical Digest (April 2, 1992), p. 1.
- <sup>2</sup> C. Umemoto and K. Takahashi, "Imeijingu pureito san gata no kijintokusei to gashitsu," Phosphor Research Society (of Japan) 224th Meeting Technical Digest (March 3, 1989), p. 1.
- <sup>3</sup> M. Sonoda, M. Takano, J. Miyahara, and H. Kato, "Computed radiography utilizing scanning laser stimulated luminescence," *Radiology* **148**, 833–838 (1983).
- <sup>4</sup> M. D. Cohen, B. P. Kartz, L. A. Kalasinski, S. J. White, J. A. Smith, and B. Long, "Digital imaging with a photostimulable phosphor in the chest of newborns," *Radiology* **181**, 829–832 (1991).
- <sup>5</sup> R. Jenkins, R. W. Gould, and D. Gedcke, *Quantitative X-Ray Spectrometry* (Marcel Dekker, New York and Basel, 1983).
- <sup>6</sup> H. Fujita, D. Y. Tsai, T. Itoh, K. Doi, J. Morishita, K. Ueda, and A. Ohtsuka, "A simple method for determining the modulation transfer function in digital radiography," *IEEE Trans. Med. Imaging* **11**, 34–39 (1992).
- <sup>7</sup> W. Hillen W, U. Schibel, and T. Zsengel, "Imaging performance of a digital storage phosphor system," *Med. Phys.* **14**, 744–751 (1987).
- <sup>8</sup> S. M. Seltzer and J. H. Hubbell, "Tables and graphs of photon mass attenuation coefficients and mass energy-absorption coefficients for photon energies 1 keV to 20 MeV for elements  $Z=1$  to 92 and some dosimetric materials," *Koshi genjyaku keisu deita bukku* (Japanese Society of Radiological Technology, Japan, 1995), pp. 9–18.
- <sup>9</sup> R. Birch, M. Marshall, G. M. Ardran in collaboration with the Diagnostic Radiology Topic Group of the Hospital Physicists' Association, *Catalogue of Spectral Data for Diagnostic X-rays* (Hospital Physicists' Association, 1979).
- <sup>10</sup> J. T. Dobbins III, D. L. Ergun, L. Rutz, D. A. Hinshaw, H. Blume, and D. C. Clark, "DQE(f) of four generations of computed radiography acquisition devices," *Med. Phys.* **22**, 1581–1593 (1995).
- <sup>11</sup> C. D. Bradford, W. W. Peppler, and J. T. Dobbins III, "Performance characteristics of a Kodak computed radiography system," *Med. Phys.* **26**, 27–37 (1999).
- <sup>12</sup> S. M. Kengyelics, A. G. Davies, and A. R. Cowen, "A comparison of the physical imaging properties of Fuji ST-V, ST-VA, and ST-VN computed radiography image plates," *Med. Phys.* **25**, 2163–2169 (1998).